UC Santa Barbara
UC Santa Barbara Previously Published Works

Title
Interface atomic structure of epitaxial ErAs layers on (001) In0.53Ga0.47As and GaAs

Permalink
https://escholarship.org/uc/item/89w225hc

Journal
Applied Physics Letters, 86

Authors
Klenov, Dmitri O
Zide, Joshua M.
Zimmerman, Jeramy D.
et al.

Publication Date
2005

Peer reviewed

eScholarship.org Powered by the California Digital Library
University of California

Applied Physics Letters **86**, art.-no. 241901 (2005).

Interface atomic structure of epitaxial ErAs layers on (001) $In_{0.53}Ga_{0.47}As$ and GaAs

Dmitri O. Klenov [a], Joshua M. Zide, Jeramy D. Zimmerman, Arthur C. Gossard and Susanne Stemmer [b]

Materials Department, University of California, Santa Barbara, CA 93106-5050

[a] Electronic address: d.o.klenov@physics.org

[b] Electronic address: stemmer@mrl.ucsb.edu

Applied Physics Letters **86**, art.-no. 241901 (2005).

Abstract

High-angle annular dark-field (HAADF) imaging in scanning transmission electron microscopy was used to determine the atomic structure of interfaces between epitaxial ErAs layers with the cubic rock salt structure and $In_{0.53}Ga_{0.47}As$ and GaAs, respectively. All layers were grown by molecular beam epitaxy. We show that the interfacial atomic arrangement corresponds to the so-called chain model, in which the zinc blende semiconductor is terminated with a Ga layer. Image analysis was used to quantify the expansion between the first ErAs plane and the terminating Ga plane. In the HAADF images, a high intensity transfer from the heavy Er columns into the background was observed in the ErAs layer, whereas the background in $In_{0.53}Ga_{0.47}As$ was of much lower intensity.

All-epitaxial metal/semiconductor composites have attracted attention due to their unique optical, magnetic and electronic properties. For example, metal nanoparticle/semiconductor composites can be conductive or insulating [1], they show ultrafast photoconduction [2], interesting magnetotransport properties [3] and strong electron plasmon resonances [4]. These properties enable new devices, such as photomixers for solid-state THz emitters [2]. ErAs is a semimetal that has the cubic rock salt structure ($a_{ErAs} = 0.573$ nm) and is known to grow epitaxially on arsenide semiconductors with the zincblende structure [5], such as GaAs and $In_{0.53}Ga_{0.47}As$ ($a_{GaAs} = 0.56538$ nm and $a_{In_{0.53}Ga_{0.47}As} = 0.5869$ nm). The atomic structure of epitaxial layered ErAs/GaAs heterostructures and of epitaxial ErAs nanoparticle/semiconductor composites has been studied experimentally and theoretically [5-11]. For example, it has been shown that the As sublattice is continuous across the interface in both types of heterostructures [9,11]. However, the precise interface atomic structure has not yet been determined.

Two distinct models have been proposed in the literature for the structure of the rock salt/zinc blende interfaces with a continuous As sublattice [7] and are schematically depicted in Fig. 1. The difference between the two models is the termination of the III-V semiconductor, which can either end with a layer of As or a layer of the group III elements (In/Ga or Ga, respectively). The As-terminated model is known as the "shadow" model because the Er atoms are placed on top of the As atoms of the zinc blende semiconductor. The In/Ga or Ga terminated model is referred to as the chain model. In case of an As-terminated semiconductor, the chain interface can form by Er

atoms filling the As layer. In addition, interface reconstructions, relaxations and/or nonstoichiometry may occur.

In this study, high-angle annular dark-field (HAADF or Z-contrast) imaging in scanning transmission electron microscopy (STEM) is used to establish the atomic structure of $ErAs/In_{0.53}Ga_{0.47}As$ and ErAs/GaAs interfaces. Epitaxial metal nanoparticle/semiconductor composites are not suited for these studies, as the overlap between two lattices makes it impossible to distinguish between the two models, even in directly interpretable atomic structure images obtained by HAADF-STEM [9]. Therefore, all investigations were performed using epitaxial ErAs layers, deposited under similar conditions as the metal nanoparticle/semiconductor composites investigated previously [9].

Films were grown on 2” (001) semi-insulating (001) InP:Fe or (001) GaAs single crystals, respectively, by molecular beam epitaxy (MBE) using a Varian Gen II MBE system. The substrate oxide was desorbed at 560 °C – 620 °C under an As_2 overpressure. 100 nm of GaAs were grown homoepitaxially at 580 °C on the GaAs substrate. On the InP, thick (1100 nm), lattice matched ($a_{InP} = 0.5869$ nm) Si-doped $In_{0.53}Ga_{0.47}As$ layers were deposited before ErAs deposition. The Er source was a solid-source effusion cell. The growth temperatures were 530 °C (on GaAs) and 490 °C (on $In_{0.53}Ga_{0.47}As$) using an As_2 overpressure of 2×10^{-6} Torr. The thickness of the ErAs was 6 nm and 20 nm on $In_{0.53}Ga_{0.47}As$ layers and GaAs layers, respectively. The samples were in-situ capped either with Al or GaAs, respectively, to prevent oxidation of the ErAs. Cross-section transmission electron microscopy (TEM) samples were prepared by standard techniques, including Ar ion milling (Gatan PIPS). To remove damage from ion-milling, TEM foils

were etched for 1 min in a 50:1 solution of citric acid and H_2O_2, followed by plasma cleaning to reduce contamination under the small electron probe. HAADF-STEM was performed using a field-emission transmission electron microscope (FEI Tecnai F30U) operated at 300 kV, equipped with a UTWIN objective lens (coefficient of spherical aberration: Cs = 0.52 mm) and a Fischione HAADF detector.

Figure 2 shows an HAADF-STEM image of the interface between ErAs and GaAs viewed along [110]. The interface is atomically abrupt and no extended defects, such as dislocations or planar faults, are observed. In HAADF, the intensity in the columns is approximately proportional to the atomic number $Z^{1.7}$ [12] of the elements in an atom column, and the positions of Er, As and Ga columns can be determined directly from these images (see atom overlay in Figs. 2 and 3). Consistent with the previous observations [9,11], the As sublattice is found to be continuous across the interface. Along [110], a chain model interface should show triplets of Er-Ga-As columns (circled in Fig. 1(c)) alternating with As columns along the interface, whereas a shadow model interface should show Er-As dumbbells also alternating with As columns along the interface (see circle in Fig. 1 (f)). In Fig. 2, some contrast can be detected between the Er-As dumbbell at the interface and may be due to the Ga column of a chain model interface. However, the estimated spacing between the Er-Ga-As triplet in the chain model approaches the resolution of the microscope (~ 0.14 nm). Furthermore, the image contrast may be complicated by atom column relaxations at the interface. It is thus difficult to distinguish the two models by imaging the interface solely along [110].

In contrast, HAADF images along the perpendicular in-plane direction ($[1\bar{1}0]$), shown for both $In_{0.53}Ga_{0.47}As$ and GaAs in Fig. 3, clearly show that the atom arrangement

at the interface corresponds to that of the chain model. In particular, Ga (Ga-In)-As dumbbells alternate with Er columns along the interface, as expected for a chain model interface imaged along $[1\bar{1}0]$ (see circle in Fig. 1 (b)). The Ga (Ga-In) layer terminating the semiconductor (arrows in Fig 3) at the interface appears to be completely occupied. In the shadow model no such Ga layer would be present (see circle in Fig. 1(e)). The interfaces on GaAs showed greater roughness, which was anisotropic with the wavelength parallel to [110] and thus did not affect the interpretation of the image contrast parallel to $[1\bar{1}0]$.

Intensity profiles across the images (Fig. 4) show that the spacing between the As columns in the first ErAs layer and the Ga (Ga-In) columns in the last zinc blende semiconductor layer is larger than the spacing between Ga (Ga-In)-As dumbbells in the bulk semiconductor (***d*** in Figs. 1(b) and 4). This likely serves to increase the spacing between the Er atoms in the interstitial sites of the As sublattice in the first ErAs layer and the Ga (Ga-In) in the last semiconductor layer underneath it. For the unrelaxed chain model interface shown in Fig. 1, the distance between Er and Ga (Ga-In) atoms across the interface is only $a\sqrt{3}/4$ (about 0.25 nm). The average projected distance between the As columns in the first ErAs layer and the Ga (Ga-In) columns measured from the images is about 0.20 nm along the interface, which resulted in Er-Ga distances across the interface of about 0.29 ± 0.02 nm. This distance is between the Ga-Ga and Er-Er distances found in metals (0.2692 nm [13] and 0.3558 nm [14], respectively) but smaller than either Er-Er or Ga-Ga distances in rock salt or zinc blende ($a\sqrt{2}/2$). The measured expansion is in close agreement with theoretical findings [8].

It is interesting to note the increase in the background intensity (thick dashed lines) in the line profiles in Fig. 4 when the probe moves from the $In_{0.53}Ga_{0.47}As$ layer into the ErAs layer. Assuming that the TEM foil thickness is the same on both sides of the interface, it shows that due to the heavy Er (Z_{Er} = 68) columns in the ErAs there is a high amount of intensity that is not confined to the columns. The background intensity in ErAs relative to that of $In_{0.53}Ga_{0.47}As$ increased with TEM foil thickness (Fig. 4(a) and (b)). The As columns in the ErAs showed greater absolute intensities than those in GaAs or $In_{0.53}Ga_{0.47}As$ (block arrows in Fig. 4), indicating very little (if any) reduction in the signal-to-background ratio, despite the increase in background intensity. The images also showed that thin regions [Fig. 4 (b)] of the sample yielded approximately the expected ($Z^{1.7}$ approximation) intensity ratios of atom columns above the background whereas in thicker regions [Fig. 4 (a)] the Er/As intensity ratio decreased. One possible explanation for this effect is an intensity transfer from the heavier Er column to the As columns [15,16]. Such "cross-talk" has been suggested in the literature for electron probes that are comparable to the interatomic spacing [16]. In contrast, even in the thicker regions shown here [Fig. 4 (a)], the intensities ratios between In-Ga and As columns in $In_{0.53}Ga_{0.47}As$ remained close to what is expected using the $Z^{1.7}$ approximation. Thus the change in relative intensity ratios in the ErAs may be due to a small misorientation of the film or small changes in the focus condition in this part of the sample. These results show that care should be taken if, for example, occupancies of the columns near or inside the ErAs are to be analyzed based on relative image intensities. It does, however, not affect the conclusions drawn in this letter, as images were only interpreted in terms of atom positions.

In summary, we have used HAADF-STEM imaging to establish the interface atomic structure between rock salt ErAs layers and arsenic zinc blende semiconductors. The interface atomic arrangement corresponds to the chain model proposed in the literature. An increase in Ga and As spacing, relative to that in the bulk semiconductor, was observed at the interface. We have also provided experimental evidence that in crystals containing heavy elements, image intensity interpretation in terms of column occupancy may require image simulations.

The authors would like to thank Prof. Ram Seshadri of UCSB for helpful discussions. This research was supported by NSF under Award No. CHE-0434567. The work made use of the UCSB MRL central facilities supported by NSF under Awards No. DMR 00-80034 and DMR 0216466.

Applied Physics Letters **86**, art.-no. 241901 (2005).

References

1. D. C. Driscoll, M. Hanson, C. Kadow, and A. C. Gossard, J. Vac. Sci. & Technol. B **19,** 1631 (2001).
2. C. Kadow, S. B. Fleischer, J. P. Ibbetson, J. E. Bowers, A. C. Gossard, J. W. Dong, and C. J. Palmstrom, Appl. Phys. Lett. **75,** 3548 (1999).
3. S. J. Allen, N. Tabatabaie, C. J. Palmstrom, G. W. Hull, T. Sands, F. Derosa, H. L. Gilchrist, and K. C. Garrison, Phys. Rev. Lett. **62,** 2309 (1989).
4. E. R. Brown, A. Bacher, D. Driscoll, M. Hanson, C. Kadow, and A. C. Gossard, Phys. Rev. Lett. **90** (2003).
5. C. J. Palmstrom, N. Tabatabaie, and S. J. Allen, Appl. Phys. Lett. **53,** 2608 (1988).
6. A. Guivarch, Y. Ballini, M. Minier, B. Guenais, G. Dupas, G. Ropars, and A. Regreny, J. Appl. Phys. **73,** 8221 (1993).
7. E. Tarnow, J. Appl. Phys. **77,** 6317 (1995).
8. W. R. L. Lambrecht, A. G. Ptukhov, and B. T. Hemmelman, Solid State Commun. **108,** 361 (1998).
9. D. O. Klenov, D. C. Driscoll, A. C. Gossard, and S. Stemmer, submitted to Appl. Phys. Lett. (manuscript number #L04-6051) (2005).
10. J. G. Zhu, C. J. Palmstrom, and C. B. Carter, Acta Metall. Mater. **43,** 4171 (1995).
11. N. G. Stoffel, C. J. Palmstrom, and B. J. Wilkens, Nuclear Instrum. & Methods Phys. Res. B **56-7,** 792 (1991).
12. E. J. Kirkland, R. F. Loane, and J. Silcox, Ultramicroscopy **23,** 77 (1987).
13. B. D. Sharma and J. Donohue, Z. Kristallogr. **117,** 293 (1962).

Applied Physics Letters **86**, art.-no. 241901 (2005).

14. F. H. Spedding, A. H. Daane, and K. W. Herrmann, Acta Cryst. **9,** 559 (1956).

15. L. J. Allen, S. D. Findlay, M. P. Oxley, and C. J. Rossouw, Ultramicroscopy **96,** 47 (2003).

16. S. Hillyard and J. Silcox, Ultramicroscopy **58,** 6 (1995).

FIGURE CAPTIONS

Figure 1 (color online)

Schematic representation of the two possible ErAs/I $In_{0.53}Ga_{0.47}As$ (GaAs) interfaces: (a-c) chain model and (d-f) shadow model, viewed along $[1\bar{1}0]$ (b, e) and [110] (c, f), respectively. The spacing labeled "*d*" marks the spacing between the last In-Ga column and the As column in the first ErAs layer.

Figure 2 (color online)

HAADF/STEM image of the ErAs/GaAs interface viewed along [110]. The overlay represents atomic column positions consistent with the chain model and the observed image contrast. Large blue disks represent As and small red and yellow disks represent Er and Ga, respectively.

Figure 3 (color online)

HAADF/STEM image of (a) the ErAs/$In_{0.53}Ga_{0.47}As$ and (b) the ErAs/GaAs viewed along $[1\bar{1}0]$, i.e., perpendicular to the viewing direction in Fig. 2. The overlay in (a) shows the atomic column positions identified from the image. Arrows mark the positions of the last row of Ga (Ga-In) atoms in the zinc blende semiconductor.

Figure 4 (color online)

Intensity profiles (averaged over a 0.05 nm wide area) across HAADF/STEM images of ErAs/$In_{0.53}Ga_{0.47}As$ interfaces recorded from different regions of the TEM sample. The

background (thick dashed lines) is greater in the ErAs relative to the $In_{0.53}Ga_{0.47}As$. The block arrows indicate the positions of As-columns. The column spacing labeled "*d*" marks the spacing between the last In-Ga column and the As column in the first ErAs layer [see also Fig. 1(b)]. (a) thicker sample region, showing an Er/As column intensity ratio of about 2.9 and (b) thinner region that shows an intensity ratio of Er/As columns close to 3.4. The expected intensity ratio is 3.4, if the image intensity is proportional to $Z^{1.7}$.

Figure 1

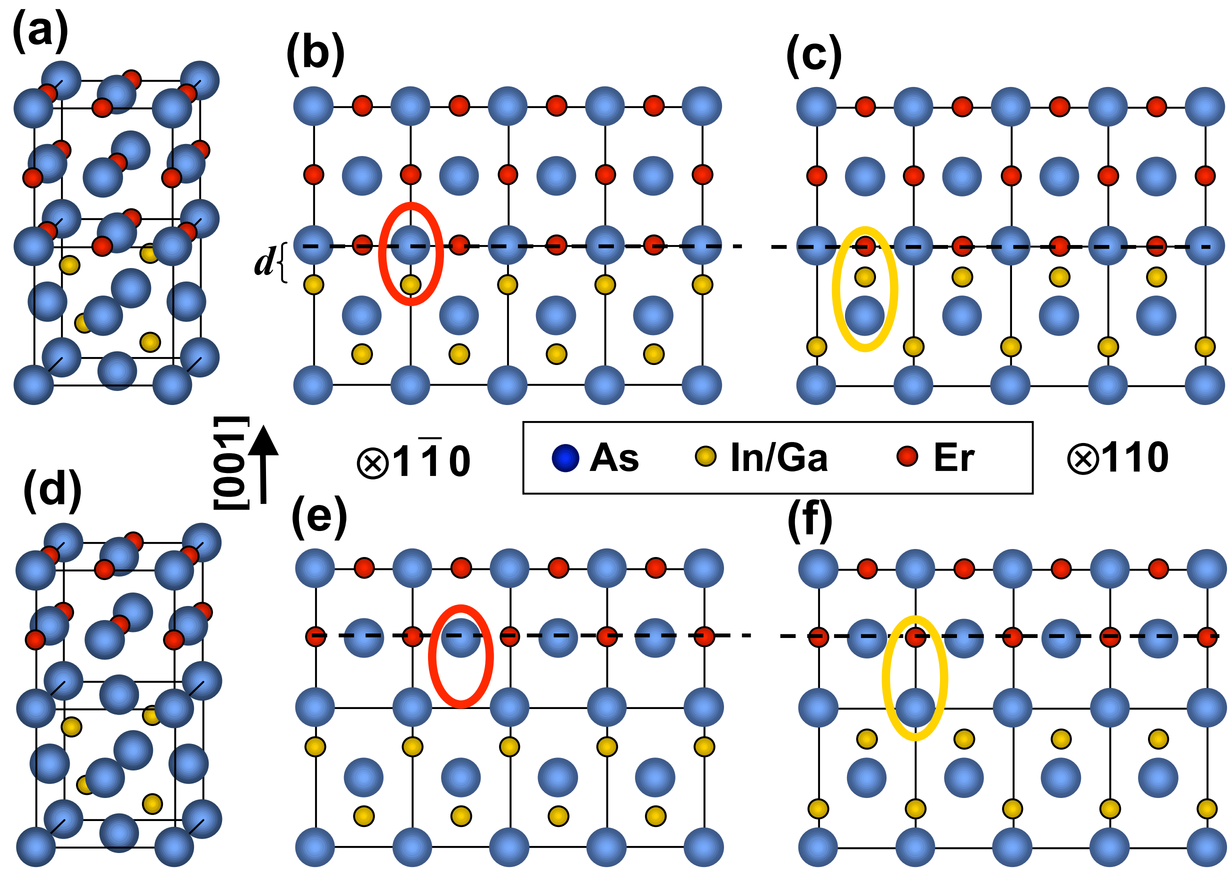

Figure 2

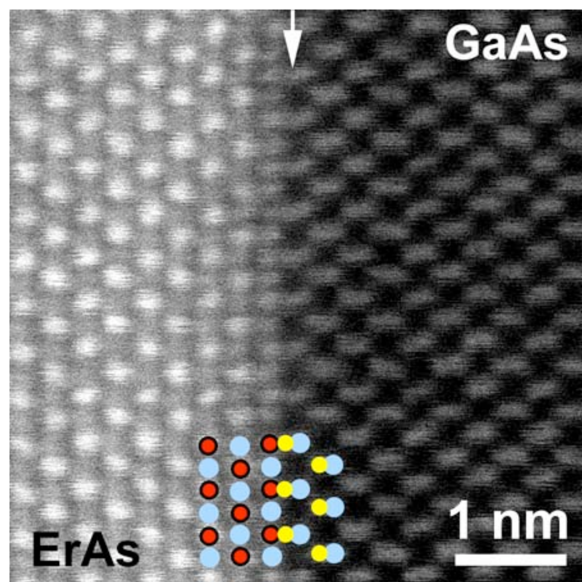

Figure 3

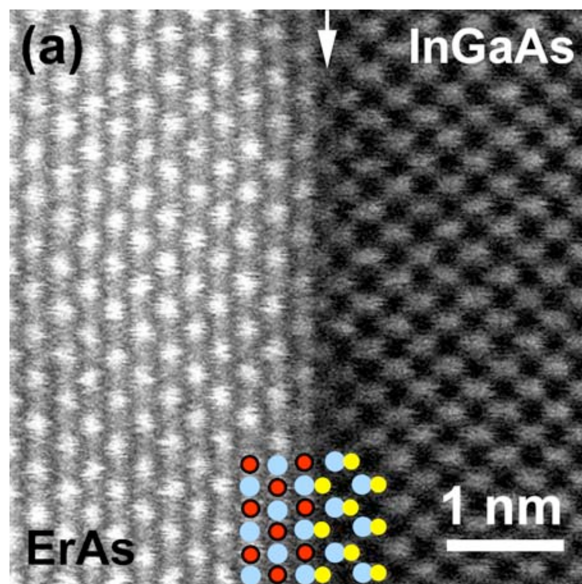

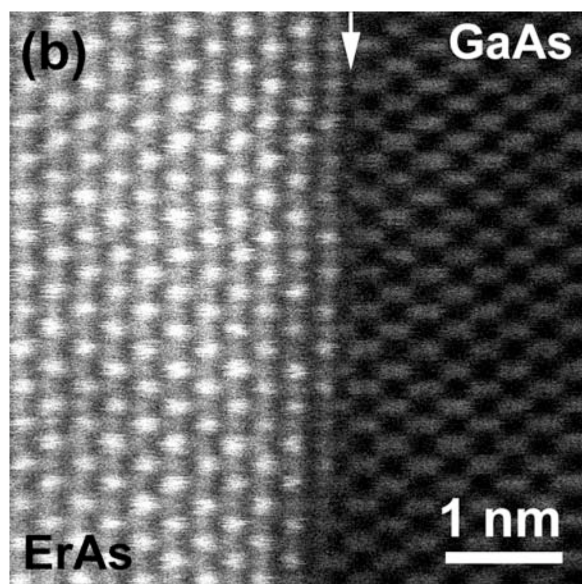

Figure 4